Observation of psi(3686) -> e(+)e(-)chi(cJ) and chi(cJ) -> e(+)e(-)J/psi

Haddadi, Z.; Kalantar-Nayestanaki, N.; Kavatsyuk, M.; Löhner, H.; Messchendorp, J.; Tiemens, M.; BESIII Collaboration

Published in:
Physical Review Letters

DOI:
10.1103/PhysRevLett.118.221802

Publication date:
2017

Observation of $\psi(3686) \to e^+e^-\chi_{cJ}$ and $\chi_{cJ} \to e^+e^-J/\psi$

M. Ablikim,[1] M. N. Achasov,[9,e] X. C. Ai,[1] O. Albayrak,[5] M. Albrecht,[4] D. J. Ambrose,[44] A. Amoroso,[49a,49c] F. F. An,[1] Q. An,[46,a] J. Z. Bai,[1] R. Baldini Ferroli,[20a] Y. Ban,[31] D. W. Bennett,[19] J. V. Bennett,[5] M. Bertani,[20a] D. Bettoni,[21a] J. M. Bian,[43] F. Bianchi,[49a,49c] E. Boger,[23,c] I. Boyko,[23] R. A. Briere,[5] H. Cai,[51] X. Cai,[1,a] O. Cakir,[40a] A. Calcaterra,[20a] G. F. Cao,[1] S. A. Cetin,[40b] J. F. Chang,[1,a] G. Chelkov,[23,c,d] G. Chen,[1] H. S. Chen,[1] H. Y. Chen,[2] J. C. Chen,[1] M. L. Chen,[1,a] S. Chen,[41] S. J. Chen,[29] X. Chen,[1,a] X. R. Chen,[26] Y. B. Chen,[1,a] H. P. Cheng,[17] X. K. Chu,[31] G. Cibinetto,[21a] H. L. Dai,[1,a] J. P. Dai,[34] A. Dbeyssi,[14] D. Dedovich,[23] Z. Y. Deng,[1] A. Denig,[22] I. Denysenko,[23] M. Destefanis,[49a,49c] F. De Mori,[49a,49c] Y. Ding,[27] C. Dong,[30] J. Dong,[1,a] L. Y. Dong,[1] M. Y. Dong,[1,a] Z. L. Dou,[29] S. X. Du,[53] P. F. Duan,[1] J. Z. Fan,[39] J. Fang,[1,a] S. S. Fang,[1] X. Fang,[46,a] Y. Fang,[1] R. Farinelli,[21a,21b] L. Fava,[49b,49c] O. Fedorov,[23] F. Feldbauer,[22] G. Felici,[20a] C. Q. Feng,[46,a] E. Fioravanti,[21a] M. Fritsch,[14,22] C. D. Fu,[1] Q. Gao,[1] X. L. Gao,[46,a] X. Y. Gao,[2] Y. Gao,[39] Z. Gao,[46,a] I. Garzia,[21a] K. Goetzen,[10] L. Gong,[30] W. X. Gong,[1,a] W. Gradl,[22] M. Greco,[49a,49c] M. H. Gu,[1,a] Y. T. Gu,[12] Y. H. Guan,[1] A. Q. Guo,[1] L. B. Guo,[28] R. P. Guo,[1] Y. Guo,[1] Y. P. Guo,[22] Z. Haddadi,[25] A. Hafner,[22] S. Han,[51] X. Q. Hao,[15] F. A. Harris,[42] K. L. He,[1] T. Held,[4] Y. K. Heng,[1,a] Z. L. Hou,[1] C. Hu,[28] H. M. Hu,[1] J. F. Hu,[49a,49c] T. Hu,[1,a] Y. Hu,[1] G. S. Huang,[46,a] J. S. Huang,[15] X. T. Huang,[33] X. Z. Huang,[29] Y. Huang,[29] Z. L. Huang,[27] T. Hussain,[48] Q. Ji,[1] Q. P. Ji,[30] X. B. Ji,[1] X. L. Ji,[1,a] L. W. Jiang,[51] X. S. Jiang,[1,a] X. Y. Jiang,[30] J. B. Jiao,[33] Z. Jiao,[17] D. P. Jin,[1,a] S. Jin,[1] T. Johansson,[50] A. Julin,[43] N. Kalantar-Nayestanaki,[25] X. L. Kang,[1] X. S. Kang,[30] M. Kavatsyuk,[25] B. C. Ke,[5] P. Kiese,[22] R. Kliemt,[14] B. Kloss,[22] O. B. Kolcu,[40b,h] B. Kopf,[4] M. Kornicer,[42] A. Kupsc,[50] W. Kühn,[24] J. S. Lange,[24] M. Lara,[19] P. Larin,[14] C. Leng,[49c] C. Li,[50] Cheng Li,[46,a] D. M. Li,[53] F. Li,[1,a] F. Y. Li,[31] G. Li,[1] H. B. Li,[1] H. J. Li,[1] J. C. Li,[1] Jin Li,[32] K. Li,[33] K. Li,[13] Lei Li,[3] P. R. Li,[41] Q. Y. Li,[33] T. Li,[33] W. D. Li,[1] W. G. Li,[1] X. L. Li,[33] X. N. Li,[1,a] X. Q. Li,[30] Y. B. Li,[2] Z. B. Li,[38] H. Liang,[46,a] Y. F. Liang,[36] Y. T. Liang,[24] G. R. Liao,[11] D. X. Lin,[14] B. Liu,[34] B. J. Liu,[1] C. X. Liu,[1] D. Liu,[46,a] F. H. Liu,[35] Fang Liu,[1] Feng Liu,[6] H. B. Liu,[12] H. H. Liu,[16] H. H. Liu,[1] H. M. Liu,[1] J. Liu,[1] J. B. Liu,[46,a] J. P. Liu,[51] J. Y. Liu,[1] K. Liu,[39] K. Y. Liu,[27] L. D. Liu,[31] P. L. Liu,[1,a] Q. Liu,[41] S. B. Liu,[46,a] X. Liu,[26] Y. B. Liu,[30] Z. A. Liu,[1,a] Zhiqing Liu,[22] H. Loehner,[25] X. C. Lou,[1,a,g] H. J. Lu,[17] J. G. Lu,[1,a] Y. Lu,[1] Y. P. Lu,[1,a] C. L. Luo,[28] M. X. Luo,[52] T. Luo,[42] X. L. Luo,[1,a] X. R. Lyu,[41] F. C. Ma,[27] H. L. Ma,[1] L. L. Ma,[33] M. M. Ma,[1] Q. M. Ma,[1] T. Ma,[1] X. N. Ma,[30] X. Y. Ma,[1,a] Y. M. Ma,[33] F. E. Maas,[14] M. Maggiora,[49a,49c] Y. J. Mao,[31] Z. P. Mao,[1] S. Marcello,[49a,49c] J. G. Messchendorp,[25] J. Min,[1,a] R. E. Mitchell,[19] X. H. Mo,[1,a] Y. J. Mo,[6] C. Morales Morales,[14] N. Yu. Muchnoi,[9,e] H. Muramatsu,[43] Y. Nefedov,[23] F. Nerling,[14] I. B. Nikolaev,[9,e] Z. Ning,[1,a] S. Nisar,[8] S. L. Niu,[1,a] X. Y. Niu,[1] S. L. Olsen,[32] Q. Ouyang,[1,a] S. Pacetti,[20b] Y. Pan,[46,a] P. Patteri,[20a] M. Pelizaeus,[4] H. P. Peng,[46,a] K. Peters,[10] J. Pettersson,[50] J. L. Ping,[28] R. G. Ping,[1] R. Poling,[43] V. Prasad,[1] H. R. Qi,[2] M. Qi,[29] S. Qian,[1,a] C. F. Qiao,[41] L. Q. Qin,[33] N. Qin,[51] X. S. Qin,[1] Z. H. Qin,[1,a] J. F. Qiu,[1] K. H. Rashid,[48] C. F. Redmer,[22] M. Ripka,[22] G. Rong,[1] Ch. Rosner,[14] X. D. Ruan,[12] A. Sarantsev,[23,f] M. Savrié,[21b] K. Schoenning,[50] S. Schumann,[22] W. Shan,[31] M. Shao,[46,a] C. P. Shen,[2] P. X. Shen,[30] X. Y. Shen,[1] H. Y. Sheng,[1] M. Shi,[1] W. M. Song,[1] X. Y. Song,[1] S. Sosio,[49a,49c] S. Spataro,[49a,49c] G. X. Sun,[1] J. F. Sun,[15] S. S. Sun,[1] X. H. Sun,[1] Y. J. Sun,[46,a] Y. Z. Sun,[1] Z. J. Sun,[1,a] Z. T. Sun,[19] C. J. Tang,[36] X. Tang,[1] I. Tapan,[40c] E. H. Thorndike,[44] M. Tiemens,[25] M. Ullrich,[24] I. Uman,[40d] G. S. Varner,[42] B. Wang,[30] B. L. Wang,[41] D. Wang,[31] D. Y. Wang,[31] K. Wang,[1,a] L. L. Wang,[1] L. S. Wang,[1] M. Wang,[33] P. Wang,[1] P. L. Wang,[1] S. G. Wang,[31] W. Wang,[1,a] W. P. Wang,[46,a] X. F. Wang,[39] Y. Wang,[37] Y. D. Wang,[14] Y. F. Wang,[1,a] Y. Q. Wang,[22] Z. Wang,[1,a] Z. G. Wang,[1,a] Z. H. Wang,[46,a] Z. Y. Wang,[1] Z. Y. Wang,[1] T. Weber,[22] D. H. Wei,[11] J. B. Wei,[31] P. Weidenkaff,[22] S. P. Wen,[1] U. Wiedner,[4] M. Wolke,[50] L. H. Wu,[1] L. J. Wu,[1] Z. Wu,[1,a] L. Xia,[46,a] L. G. Xia,[39] Y. Xia,[18] D. Xiao,[1] H. Xiao,[47] Z. J. Xiao,[28] Y. G. Xie,[1,a] Q. L. Xiu,[1,a] G. F. Xu,[1] J. J. Xu,[1] L. Xu,[1] Q. J. Xu,[13] Q. N. Xu,[41] X. P. Xu,[37] L. Yan,[49a,49c] W. B. Yan,[46,a] W. C. Yan,[46,a] Y. H. Yan,[18] H. J. Yang,[34] H. X. Yang,[1] L. Yang,[51] Y. X. Yang,[11] M. Ye,[1,a] M. H. Ye,[7] J. H. Yin,[1] B. X. Yu,[1,a] C. X. Yu,[30] J. S. Yu,[26] C. Z. Yuan,[1] W. L. Yuan,[29] Y. Yuan,[1] A. Yuncu,[40b,b] A. A. Zafar,[48] A. Zallo,[20a] Y. Zeng,[18] Z. Zeng,[46,a] B. X. Zhang,[1] B. Y. Zhang,[1,a] C. Zhang,[29] C. C. Zhang,[1] D. H. Zhang,[1] H. H. Zhang,[38] H. Y. Zhang,[1,a] J. Zhang,[1] J. J. Zhang,[1] J. L. Zhang,[1,*] J. Q. Zhang,[1] J. W. Zhang,[1,a] J. Y. Zhang,[1] J. Z. Zhang,[1] K. Zhang,[1] L. Zhang,[1] S. Q. Zhang,[30] X. Y. Zhang,[33] Y. Zhang,[1] Y. H. Zhang,[1,a] Y. N. Zhang,[41] Y. T. Zhang,[46,a] Yu Zhang,[41] Z. H. Zhang,[6] Z. P. Zhang,[46] Z. Y. Zhang,[51] G. Zhao,[1] J. W. Zhao,[1,a] J. Y. Zhao,[1] J. Z. Zhao,[1,a] Lei Zhao,[46,a] Ling Zhao,[1] M. G. Zhao,[30] Q. Zhao,[1] Q. W. Zhao,[1] S. J. Zhao,[53] T. C. Zhao,[1] Y. B. Zhao,[1,a] Z. G. Zhao,[46,a] A. Zhemchugov,[23,c] B. Zheng,[47] J. P. Zheng,[1,a] W. J. Zheng,[33] Y. H. Zheng,[41] B. Zhong,[28] L. Zhou,[1,a] X. Zhou,[51] X. K. Zhou,[46,a] X. R. Zhou,[46,a] X. Y. Zhou,[1] K. Zhu,[1] K. J. Zhu,[1,a] S. Zhu,[1] S. H. Zhu,[45] X. L. Zhu,[39] Y. C. Zhu,[46,a] Y. S. Zhu,[1] Z. A. Zhu,[1] J. Zhuang,[1,a] L. Zotti,[49a,49c] B. S. Zou,[1] and J. H. Zou[1]

(BESIII Collaboration)

[1]Institute of High Energy Physics, Beijing 100049, People's Republic of China
[2]Beihang University, Beijing 100191, People's Republic of China
[3]Beijing Institute of Petrochemical Technology, Beijing 102617, People's Republic of China
[4]Bochum Ruhr-University, D-44780 Bochum, Germany
[5]Carnegie Mellon University, Pittsburgh, Pennsylvania 15213, USA
[6]Central China Normal University, Wuhan 430079, People's Republic of China
[7]China Center of Advanced Science and Technology, Beijing 100190, People's Republic of China
[8]COMSATS Institute of Information Technology, Lahore, Defence Road, Off Raiwind Road, 54000 Lahore, Pakistan
[9]G.I. Budker Institute of Nuclear Physics SB RAS (BINP), Novosibirsk 630090, Russia
[10]GSI Helmholtzcentre for Heavy Ion Research GmbH, D-64291 Darmstadt, Germany
[11]Guangxi Normal University, Guilin 541004, People's Republic of China
[12]GuangXi University, Nanning 530004, People's Republic of China
[13]Hangzhou Normal University, Hangzhou 310036, People's Republic of China
[14]Helmholtz Institute Mainz, Johann-Joachim-Becher-Weg 45, D-55099 Mainz, Germany
[15]Henan Normal University, Xinxiang 453007, People's Republic of China
[16]Henan University of Science and Technology, Luoyang 471003, People's Republic of China
[17]Huangshan College, Huangshan 245000, People's Republic of China
[18]Hunan University, Changsha 410082, People's Republic of China
[19]Indiana University, Bloomington, Indiana 47405, USA
[20a]INFN Laboratori Nazionali di Frascati, I-00044 Frascati, Italy
[20b]INFN and University of Perugia, I-06100 Perugia, Italy
[21a]INFN Sezione di Ferrara, I-44122 Ferrara, Italy
[21b]University of Ferrara, I-44122 Ferrara, Italy
[22]Johannes Gutenberg University of Mainz, Johann-Joachim-Becher-Weg 45, D-55099 Mainz, Germany
[23]Joint Institute for Nuclear Research, 141980 Dubna, Moscow region, Russia
[24]Justus-Liebig-Universitaet Giessen, II. Physikalisches Institut, Heinrich-Buff-Ring 16, D-35392 Giessen, Germany
[25]KVI-CART, University of Groningen, NL-9747 AA Groningen, Netherlands
[26]Lanzhou University, Lanzhou 730000, People's Republic of China
[27]Liaoning University, Shenyang 110036, People's Republic of China
[28]Nanjing Normal University, Nanjing 210023, People's Republic of China
[29]Nanjing University, Nanjing 210093, People's Republic of China
[30]Nankai University, Tianjin 300071, People's Republic of China
[31]Peking University, Beijing 100871, People's Republic of China
[32]Seoul National University, Seoul, 151-747 Korea
[33]Shandong University, Jinan 250100, People's Republic of China
[34]Shanghai Jiao Tong University, Shanghai 200240, People's Republic of China
[35]Shanxi University, Taiyuan 030006, People's Republic of China
[36]Sichuan University, Chengdu 610064, People's Republic of China
[37]Soochow University, Suzhou 215006, People's Republic of China
[38]Sun Yat-Sen University, Guangzhou 510275, People's Republic of China
[39]Tsinghua University, Beijing 100084, People's Republic of China
[40a]Ankara University, 06100 Tandogan, Ankara, Turkey
[40b]Istanbul Bilgi University, 34060 Eyup, Istanbul, Turkey
[40c]Uludag University, 16059 Bursa, Turkey
[40d]Near East University, Nicosia, North Cyprus, Mersin 10, Turkey
[41]University of Chinese Academy of Sciences, Beijing 100049, People's Republic of China
[42]University of Hawaii, Honolulu, Hawaii 96822, USA
[43]University of Minnesota, Minneapolis, Minnesota 55455, USA
[44]University of Rochester, Rochester, New York 14627, USA
[45]University of Science and Technology Liaoning, Anshan 114051, People's Republic of China
[46]University of Science and Technology of China, Hefei 230026, People's Republic of China
[47]University of South China, Hengyang 421001, People's Republic of China
[48]University of the Punjab, Lahore-54590, Pakistan
[49a]University of Turin, I-10125 Turin, Italy
[49b]University of Eastern Piedmont, I-15121 Alessandria, Italy
[49c]INFN, I-10125 Turin, Italy
[50]Uppsala University, Box 516, SE-75120 Uppsala, Sweden
[51]Wuhan University, Wuhan 430072, People's Republic of China
[52]Zhejiang University, Hangzhou 310027, People's Republic of China
[53]Zhengzhou University, Zhengzhou 450001, People's Republic of China

(Received 19 January 2017; revised manuscript received 9 May 2017; published 30 May 2017)

Using 4.479×10^8 $\psi(3686)$ events collected with the BESIII detector, we search for the decays $\psi(3686) \to e^+e^-\chi_{cJ}$ and $\chi_{cJ} \to e^+e^-J/\psi$, where $J = 0, 1, 2$. The decays $\psi(3686) \to e^+e^-\chi_{cJ}$ and $\chi_{cJ} \to e^+e^-J/\psi$ are observed for the first time. The measured branching fractions are $\mathcal{B}(\psi(3686) \to e^+e^-\chi_{cJ}) = (11.7 \pm 2.5 \pm 1.0) \times 10^{-4}$, $(8.6 \pm 0.3 \pm 0.6) \times 10^{-4}$, $(6.9 \pm 0.5 \pm 0.6) \times 10^{-4}$ for $J = 0, 1, 2$, and $\mathcal{B}(\chi_{cJ} \to e^+e^-J/\psi) = (1.51 \pm 0.30 \pm 0.13) \times 10^{-4}$, $(3.73 \pm 0.09 \pm 0.25) \times 10^{-3}$, $(2.48 \pm 0.08 \pm 0.16) \times 10^{-3}$ for $J = 0, 1, 2$, respectively. The ratios of the branching fractions $\mathcal{B}(\psi(3686) \to e^+e^-\chi_{cJ})/\mathcal{B}(\psi(3686) \to \gamma\chi_{cJ})$ and $\mathcal{B}(\chi_{cJ} \to e^+e^-J/\psi)/\mathcal{B}(\chi_{cJ} \to \gamma J/\psi)$ are also reported. Also, the α values of helicity angular distributions of the e^+e^- pair are determined for $\psi(3686) \to e^+e^-\chi_{c1,2}$ and $\chi_{c1,2} \to e^+e^-J/\psi$.

DOI: 10.1103/PhysRevLett.118.221802

The study of electromagnetic (EM) Dalitz decays [1], in which a virtual photon is internally converted into an e^+e^- pair, plays an important role in revealing the structure of hadrons and the interactions between photons and hadrons [2]. Such decays are widely observed in the light-quark meson sector, for example, $\eta' \to \gamma e^+e^-$, $\eta' \to \omega e^+e^-$, and $\phi \to \eta e^+e^-$ [3]. However, the analogous transitions in charmonium decays have not yet been studied. Although the potential quark model has successfully described the low-lying charmonium states with high precisions, there are still puzzling discrepancies in the decay branching fractions $\mathcal{B}(\psi(3686) \to \gamma\chi_{cJ})$ between the experimental results [3] where the higher-order multipole amplitudes are ignored and the various theoretical predictions [4–7]. Throughout this Letter, χ_{cJ} refers to $\chi_{c0,1,2}$. While recently the BESIII experiment confirms that the contributions from the higher-order multipole amplitudes in $\psi(3686) \to \gamma\chi_{cJ}$ are small [8], the E1 contribution is dominant. Therefore, it is of great interest to measure the EM transition $\psi(3686) \to e^+e^-\chi_{cJ}$ and $\chi_{cJ} \to e^+e^-J/\psi$.

The EM Dalitz decays in charmonium transitions, such as $\psi(3686) \to e^+e^-\chi_{cJ}$ or $\chi_{cJ} \to e^+e^-J/\psi$, have access to the EM transition form factors (TFFs) of these charmonium states. The q^2 dependence of charmonium TFFs can provide additional information on the interactions between the charmonium states and the electromagnetic field, where q^2 is the square of the invariant mass of the e^+e^- pair, and serve as a sensitive probe to their internal structures. Furthermore, the q^2-dependent TFF can possibly distinguish the transition mechanisms based on the $c\bar{c}$ scenario and other solutions which alter the simple quark model picture. We emphasize that the q^2-dependent TFF can also serve as a useful probe for exotic hadron structures based on different models. One example is that with the precise measurement of the radiative decay of $X(3872) \to e^+e^-J/\psi$ and $X(3872) \to e^+e^-\psi(3686)$ in the future, we can pin down the intrinsic structure of $X(3872)$ by comparing the experimental measurement of the q^2 dependence of TFF with different model calculations. The nature of $X(3872)$, namely, whether it is a compact charmonium, multiquark state with quark clustering, or hadronic molecule [9–13], can possibly be disentangled by the q^2 dependence of its TFF.

In this Letter, we report the observation of the EM Dalitz decays $\psi(3686) \to e^+e^-\chi_{cJ}$ and $\chi_{cJ} \to e^+e^-J/\psi$ by analyzing the cascade decays $\psi(3686) \to e^+e^-\chi_{cJ}$, $\chi_{cJ} \to \gamma J/\psi$ and $\psi(3686) \to \gamma\chi_{cJ}$, $\chi_{cJ} \to e^+e^-J/\psi$, respectively. Here, the J/ψ is reconstructed in its decay to an e^+e^- or $\mu^+\mu^-$ pair. The two cascade decays studied have the same final state: four leptons and a single photon. The analysis uses a data sample of 4.479×10^8 $\psi(3686)$ events [14,15] taken at a center-of-mass energy $\sqrt{s} = 3.686$ GeV collected with the BESIII detector [16] operating at the BEPCII [17] storage ring in 2009 and 2012. In addition, a data sample corresponding to an integrated luminosity of 44 pb^{-1}, taken at a center-of-mass energy $\sqrt{s} = 3.65$ GeV [18], is used to estimate the background from continuum processes.

The BESIII detector [16] has a geometrical acceptance of 93% of the total 4π solid angle. A small-cell helium-based main drift chamber (MDC) provides momentum measurements of charged particles with resolution of 0.5% at 1 GeV$/c$. The MDC also supplies an energy loss (dE/dx) measurement with a resolution better than 6% for electrons from Bhabha scattering. The time-of-flight system (TOF) is composed of plastic scintillators with a time resolution of 80 (110) ps in the barrel (end caps) and is used for charged particle identification. The CsI(Tl) electromagnetic calorimeter (EMC) measures 1 GeV energy photons with a resolution of 2.5% (5%) in the barrel (end caps) region.

Monte Carlo (MC) simulations are used to estimate the reconstruction efficiencies and study the backgrounds. The signal MC samples are generated using EVTGEN [19] using a q^2-dependent decay amplitude based on the assumption of a pointlike meson, as described in Ref. [20], and an angular distribution based on that observed in data. An MC sample of generic $\psi(3686)$ decays, the so called "inclusive MC sample," is used for the background studies. The production of the $\psi(3686)$ state is simulated by the KKMC [21] generator. The known decay modes of the $\psi(3686)$ are simulated by EVTGEN [19] according to the branching fractions reported in PDG [3], while the unknown modes are simulated using the LUNDCHARM [22] model.

Each charged track is required to have a point of closest approach to the interaction point (IP) that is less than 1 cm in the radial direction and less than 10 cm along the beam direction. The polar angle θ of the tracks must be within the fiducial volume of the MDC ($|\cos\theta| < 0.93$). Photons are reconstructed from isolated showers in the EMC which are at least 20° away from the nearest charged track. The photon energy is required to be at least 25 MeV in the barrel region ($|\cos\theta| < 0.8$) or 50 MeV in the end cap region ($0.86 < |\cos\theta| < 0.92$). In order to suppress electronic noise and energy depositions unrelated to the event, the time after the collision at which the photon is recorded in the EMC must be less than 700 ns.

Candidate events are required to have four charged tracks, with a sum of charges equal to zero, and at least one photon. The tracks with momentum larger than 1 GeV/c are assumed to be leptons from J/ψ decay. Otherwise, they are considered as electrons from the ψ' or χ_{cJ} decay. Leptons from the J/ψ decay with EMC energy larger than 0.8 GeV are identified as electrons, otherwise as muons. The J/ψ signal is identified by requiring the invariant mass of the lepton pair to be in the interval [3.08, 3.12] GeV/c^2. A vertex fit is performed on the four charged tracks to ensure the tracks originated from the IP. In order to reduce the background and improve the mass resolution, a four-constraint (4C) kinematic fit is performed by constraining the total four momentum to that of the initial beams. If there is more than one photon candidate in an event, all the photons are individually fit with the four leptons in the kinematic fit and only those with a fit $\chi^2 < 40$ are retained. If two or more photons pass this criterion, only the one with the least χ^2 is retained for further analysis.

A study of the $\psi(3686)$ inclusive MC sample shows that, after applying the above selection criteria, the main background comes from $\psi(3686) \to \gamma\chi_{cJ}, \chi_{cJ} \to \gamma J/\psi$ decays, where one photon converts into an e^+e^- pair in the detector material. To suppress this background, a photon-conversion finder [23] is applied to reconstruct the photon-conversion vertex. The distance from the point of the reconstructed conversion vertex to the z axis, R_{xy}, is used to distinguish the photon conversion background from signal. By studying the MC samples $\psi(3686) \to \gamma\chi_{cJ}$, $\chi_{cJ} \to \gamma J/\psi$, the peaks around $R_{xy} = 3$ and $R_{xy} = 6$ cm match the positions of the beam pipe and the inner wall of the MDC [16], respectively. We remove the events in 1.5 cm $< R_{xy} <$ 7.5 cm to suppress the γ conversion background. With this requirement, the γ conversion background is negligible for the decays $\psi(3686) \to e^+e^-\chi_{cJ}$ and is at the few percent level for the decays $\chi_{cJ} \to e^+e^-J/\psi$.

To remove the backgrounds from decays $\psi(3686) \to \eta/\pi^0 J/\psi, \eta/\pi^0 \to \gamma e^+e^-$, which have the same final state as signal events, a requirement $0.16 < M(\gamma e^+e^-) <$ 0.50 GeV/c^2 is applied. By studying the data collected at $\sqrt{s} = 3.65$ GeV, the contribution from the continuum process is found to be negligible.

Figure 1 shows the scatter plot of $M(\gamma J/\psi)$ versus $M(e^+e^-J/\psi)$ for the selected events from data; the corresponding one-dimensional projections are shown in

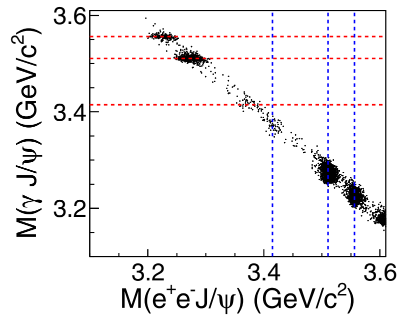

FIG. 1. Scatter plot of $M(\gamma J/\psi)$ versus $M(e^+e^-J/\psi)$ for data. The horizontal red dashed lines and vertical blue dashed lines indicate the positions of the χ_{cJ} masses in the $M(\gamma J/\psi)$ and $M(e^+e^-J/\psi)$ distributions, respectively.

Fig. 2. Clear χ_{cJ} signals are observed in the $M(\gamma J/\psi)$ and $M(e^+e^-J/\psi)$ distributions, corresponding to the decays $\psi(3686) \to e^+e^-\chi_{cJ}$ and $\chi_{cJ} \to e^+e^-J/\psi$, respectively. The study of $\psi(3686)$ inclusive MC samples indicates that the dominant background is from the decay $\psi(3686) \to \pi^+\pi^-J/\psi$, $J/\psi \to (\gamma_{\rm FSR})l^+l^-$, where $\gamma_{\rm FSR}$ is a photon due to final-state radiation; these events accumulate at $M(e^+e^-J/\psi) \sim 3.6$ GeV/c^2.

Separate unbinned maximum likelihood fits are performed on the $M(\gamma J/\psi)$ and $M(e^+e^-J/\psi)$ distributions to extract the signal yields. We use the signal MC-determined shape, convoluted with a common Gaussian function, to describe the shapes of χ_{cJ} signals. The Gaussian function parametrizes any resolution difference between the data and MC simulation and its parameters are determined from the fit.

Two background components are considered in the fit to the $M(\gamma J/\psi)$ distribution. The first background is from the decay $\psi(3686) \to \gamma\chi_{c0}$, $\chi_{c0} \to e^+e^-J/\psi$, which corresponds to the peak at the lower edge of the $M(\gamma J/\psi)$ region; it is described by a MC-determined shape with a fixed number of events based on the branching fraction obtained in this analysis. The second one is related to QED background ($e^+e^- \to \ell^+\ell^-, \ell = e, \mu, \tau$) and is described by a first-order polynomial function in the fit.

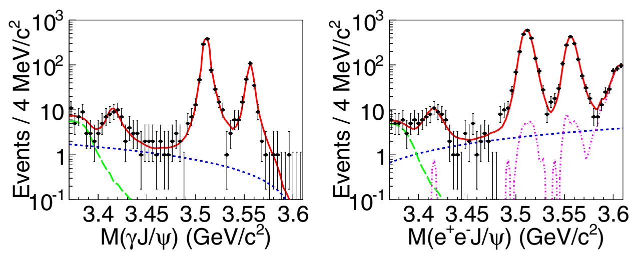

FIG. 2. Data (points with error bars) distributions of (left) $M(\gamma J/\psi)$ and (right) $M(e^+e^-J/\psi)$. The red solid curve is the overall fit result, the green long-dashed curve is for the background (left) $\psi(3686) \to \gamma\chi_{c0}$, $\chi_{c0} \to e^+e^-J/\psi$ and (right) $\psi(3686) \to e^+e^-\chi_{c0}, \chi_{c0} \to \gamma J/\psi$, the blue dashed curve is for QED background, and the pink dashed-dotted curve in right plot is for the backgrounds from $\psi(3686)$ decays.

In the fit to the $M(e^+e^-J/\psi)$ distribution, three background components are considered. The first two are from the decay $\psi(3686) \to e^+e^-\chi_{c0}, \chi_{c0} \to \gamma J/\psi$, which corresponds to the enhancement at the lower edge of the $M(e^+e^-J/\psi)$ fit interval, and QED processes; the way these components are dealt with in this fit is analogous to the way they are dealt with in the $M(\gamma J/\psi)$ fit. The third background component is from inclusive $\psi(3686)$ decay, which includes the dominant one of $\psi(3686) \to \pi^+\pi^-J/\psi$, $J/\psi \to (\gamma_{\rm FSR})l^+l^-$ decays and a small fraction from $\psi(3686) \to \gamma_1\chi_{cJ}$, $\chi_{cJ} \to \gamma_2 J/\psi$, where γ_2 converts into an e^+e^- pair. In the fit, the shape of the third background component is assumed to be that reconstructed in the inclusive MC sample with the normalization determined from data. The fit results are shown in Fig. 2 and the corresponding signal yields are summarized in Table I. For the six observed decay modes, the statistical significance of the yields are all larger than 5 standard deviations.

The branching fractions $\mathcal{B}(\psi(3686) \to e^+e^-\chi_{cJ})$ and $\mathcal{B}(\chi_{cJ} \to e^+e^-J/\psi)$ are calculated according to

$$\mathcal{B} = \frac{N_{\rm sig}}{N_{\psi(3686)}\epsilon\mathcal{B}_{\rm radiative}\mathcal{B}(J/\psi \to l^+l^-)}, \qquad (1)$$

where $N_{\rm sig}$ is the corresponding number of signal events extracted from the fit, $N_{\psi(3686)}$ is the total number of $\psi(3686)$ events, ϵ is the selection efficiency determined from the signal MC samples, $\mathcal{B}_{\rm radiative}$ is the branching fraction of the radiative transitions $\psi(3686) \to \gamma\chi_{cJ}$ or $\chi_{cJ} \to \gamma J/\psi$, and $\mathcal{B}(J/\psi \to l^+l^-)$ is the decay branching fraction of $J/\psi \to l^+l^-$. All the branching fractions used are taken from Ref. [3]. The resultant branching fractions of $\psi(3686) \to e^+e^-\chi_{cJ}$ and $\chi_{cJ} \to e^+e^-J/\psi$ are listed in Table I.

Figure 3 shows comparisons of the q distributions in data and MC simulation for the decays $\psi(3686) \to e^+e^-\chi_{c1,2}$ and $\chi_{c1,2} \to e^+e^-J/\psi$, where the χ_{c1} and χ_{c2} signals are extracted requiring a mass within [3.49,3.53] and [3.54, 3.58] GeV/c^2, respectively; with these criteria the backgrounds are expected to be less than 2%. The data are in reasonable agreement with the MC simulation generated using the model described in Ref. [20].

The systematic uncertainties for the branching fraction measurement arise from the following sources: track reconstruction, photon detection, kinematic fitting, J/ψ mass criteria, $M(\gamma e^+e^-)$ requirement, γ conversion vetoing, fit procedure, angular distributions, the total number of $\psi(3686)$ events, and the branching fractions of the cascade decays. All uncertainties are discussed in detail below.

The difference in the tracking efficiency between data and the MC simulation, for each charged track, is estimated to be 1.0% [24], which results in a 4.0% systematic uncertainty for all modes. The uncertainty on the photon-detection efficiency is derived from a control sample of $J/\psi \to \rho^0\pi^0$ decays and is 1.0% per photon [25].

In the 4C kinematic fit, the helix parameters of charged tracks are corrected to reduce the discrepancy between data and the MC simulation as described in Ref. [26]. The correction factors are obtained by studying a control sample of $\psi(3686) \to \pi^+\pi^-J/\psi, J/\psi \to l^+l^-$ decays. To determine the systematic uncertainty from this source, we determine the efficiencies from the MC samples without the helix correction; the resulting differences with respect to the nominal values are taken as the systematic uncertainties.

The uncertainty associated with the J/ψ mass requirement is 1.0%, which is determined by studying a control sample of $\psi(3686) \to \eta J/\psi$, $\eta \to \gamma\gamma$ (where one γ undergoes conversion to an e^+e^- pair) or $\eta \to \gamma e^+e^-$ decays. The systematic uncertainty related to the $M(\gamma e^+e^-)$ interval used is studied by varying the edges of the interval by ± 5 MeV/c^2. The largest difference with the nominal value is taken as the systematic uncertainty from this source.

To study the systematic uncertainty related to the γ conversion background veto, we compare the efficiencies of γ conversion veto between data and the MC simulation in control samples of $\psi(3686) \to \gamma\chi_{c1,2}$, $\chi_{c1,2} \to e^+e^-J/\psi$ decays. The efficiency of the γ conversion veto is the ratio of the signal yields determined by fitting the $M(e^+e^-)$ distribution with and without the γ conversion veto applied. A relative difference between data and simulation of 1.4% is found and assigned as the systematic uncertainty.

The sources of uncertainty in the fit procedure include the fit range and the signal and background parametrization. The uncertainty related with the fit range is obtained

TABLE I. Signal yields, detection efficiencies, the branching fractions, and the ratios of the branching fractions. Here, the first uncertainty is statistical and the second systematic.

Mode	Yields	Efficiency(%)	Branching fraction	$\mathcal{B}(\psi(3686) \to e^+e^-\chi_{cJ})/\mathcal{B}(\psi(3686) \to \gamma\chi_{cJ})$	$\mathcal{B}(\chi_{cJ} \to e^+e^-J/\psi)/\mathcal{B}(\chi_{cJ} \to \gamma J/\psi)$
$\psi(3686) \to e^+e^-\chi_{c0}$	48 ± 10	6.06	$(11.7 \pm 2.5 \pm 1.0) \times 10^{-4}$	$(9.4 \pm 1.9 \pm 0.6) \times 10^{-3}$	...
$\psi(3686) \to e^+e^-\chi_{c1}$	873 ± 30	5.61	$(8.6 \pm 0.3 \pm 0.6) \times 10^{-4}$	$(8.3 \pm 0.3 \pm 0.4) \times 10^{-3}$	...
$\psi(3686) \to e^+e^-\chi_{c2}$	227 ± 16	3.19	$(6.9 \pm 0.5 \pm 0.6) \times 10^{-4}$	$(6.6 \pm 0.5 \pm 0.4) \times 10^{-3}$	...
$\chi_{c0} \to e^+e^-J/\psi$	56 ± 11	6.95	$(1.51 \pm 0.30 \pm 0.13) \times 10^{-4}$	...	$(9.5 \pm 1.9 \pm 0.7) \times 10^{-3}$
$\chi_{c1} \to e^+e^-J/\psi$	1969 ± 46	10.35	$(3.73 \pm 0.09 \pm 0.25) \times 10^{-3}$	...	$(10.1 \pm 0.3 \pm 0.5) \times 10^{-3}$
$\chi_{c2} \to e^+e^-J/\psi$	1354 ± 39	11.23	$(2.48 \pm 0.08 \pm 0.16) \times 10^{-3}$	...	$(11.3 \pm 0.4 \pm 0.5) \times 10^{-3}$

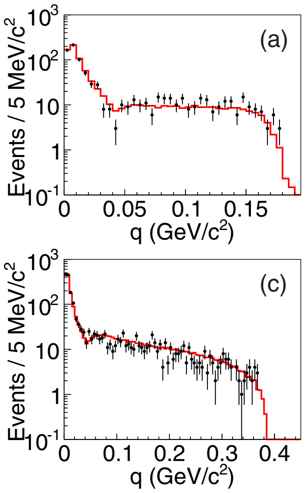

FIG. 3. Data to MC simulation comparisons of q distribution for the decays (a) $\psi(3686) \to e^+e^-\chi_{c1}$, (b) $\psi(3686) \to e^+e^-\chi_{c2}$, (c) $\chi_{c1} \to e^+e^-J/\psi$, and (d) $\chi_{c2} \to e^+e^-J/\psi$. The points with error bars are data and the red histograms are for the signal MC simulation.

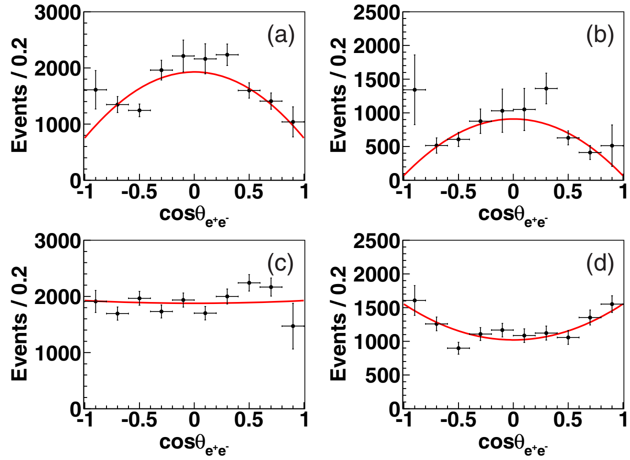

FIG. 4. Distributions of efficiency corrected $\cos\theta_{e^+e^-}$ for the decays (a) $\psi(3686) \to e^+e^-\chi_{c1}$, (b) $\psi(3686) \to e^+e^-\chi_{c2}$, (c) $\chi_{c1} \to e^+e^-J/\psi$, and (d) $\chi_{c2} \to e^+e^-J/\psi$. The red line is the fit to $1 + \alpha\cos^2\theta_{e^+e^-}$.

by varying the limits of the fit range by $\pm 5\ \mathrm{MeV}/c^2$. The largest difference in the signal yields with respect to the nominal values is taken as the systematic uncertainty. In the nominal fit, the signal shapes are described with the signal MC simulated shapes convoluted with a Gaussian function. An alternative fit is performed by fixing the signal shapes to those of MC simulation. The resultant change in the signal yields is taken as the systematic uncertainty. The uncertainty associated with the background shape is estimated by an alternative fit replacing the first order polynomial function with a second order polynomial function for the background shape, the resultant change in the signal yields is taken as the systematic uncertainty.

The distribution of e^+e^- pair's helicity angle in its mother rest frame $\theta_{e^+e^-}$ may affect the detector efficiency, where $\theta_{e^+e^-}$ is the polar angle of e^+e^- pair in the colliding beams rest frame with the z axis pointing in the positron beam direction. The efficiency corrected $\cos\theta_{e^+e^-}$ distributions are shown in Fig. 4 for the decays $\psi(3686) \to e^+e^-\chi_{c1,2}$ and $\chi_{c1,2} \to e^+e^-J/\psi$; each distribution is fit with a $1 + \alpha\cos^2\theta_{e^+e^-}$ function. The resultant α values are -0.6 ± 0.2, -0.9 ± 0.3, 0.0 ± 0.2, and 0.5 ± 0.2 for the decays $\psi(3686) \to e^+e^-\chi_{c1}$, $\psi(3686) \to e^+e^-\chi_{c2}$, $\chi_{c1} \to e^+e^-J/\psi$, and $\chi_{c2} \to e^+e^-J/\psi$, respectively. The measured α central values are incorporated in the nominal MC simulations. To take into account any effect on the detection efficiencies due to an incorrect simulation of the $\cos\theta_{e^+e^-}$ distribution, alternative MC samples are generated with α varied by ± 1 standard deviation and the efficiencies are determined. The differences with the nominal efficiencies are taken as the systematic uncertainties from this source. In the decays $\psi(3686) \to e^+e^-\chi_{c0}$ and $\chi_{c0} \to e^+e^-J/\psi$, the $\cos\theta_{e^+e^-}$ distribution is not extracted directly from the data due to the limited statistics. The theoretical expectations for α are 1 and 0 for $\psi(3686) \to e^+e^-\chi_{c0}$ and $\chi_{c0} \to e^+e^-J/\psi$, respectively, which are used to generate the nominal MC simulation. The systematic uncertainty is estimated using the difference in efficiency when alternative MC samples with $\alpha = 0$ for $\psi(3686) \to e^+e^-\chi_{c0}$ and $\alpha = 1$ for $\chi_{c0} \to e^+e^-J/\psi$ are used.

The total number of $\psi(3686)$ events is measured to within 0.7% by using the inclusive hadronic events [14,15]. The uncertainties of the branching fractions in the cascade decays are taken from Ref. [3].

The effect of other potential systematic uncertainty sources are considered, such as uncertainties on the generated q distributions, the trigger efficiency, and the simulation of the event time, but are all found to be negligible. Table II summarizes all individual systematic uncertainties, and the overall uncertainties are the quadrature sums of the individual ones, assuming they are independent.

TABLE II. Summary of systematic uncertainties (in %).

	$\psi(3686) \to e^+e^-\chi_{cJ}$			$\chi_{cJ} \to e^+e^-J/\psi$		
	χ_{c0}	χ_{c1}	χ_{c2}	χ_{c0}	χ_{c1}	χ_{c2}
Tracking	4.0	4.0	4.0	4.0	4.0	4.0
Photon	1.0	1.0	1.0	1.0	1.0	1.0
Kinematic fit	1.6	1.4	1.4	1.8	2.2	2.4
J/ψ mass window	1.0	1.0	1.0	1.0	1.0	1.0
$M(\gamma e^+e^-)$	2.7	1.2	1.0	0.7	2.2	0.4
γ conversion vetoing	1.4	1.4	1.4	1.4	1.4	1.4
Fit range	2.2	0.2	0.3	4.7	0.1	0.2
Signal shape	0.4	0.1	0.1	2.2	0.2	0.5
Background shape	2.2	0.2	0.3	0.1	0.1	0.2
Angular distribution	3.9	2.1	3.3	3.6	1.6	1.0
Number of $\psi(3686)$	0.7	0.7	0.7	0.7	0.7	0.7
Branching fractions	4.8	3.6	5.5	2.8	3.3	3.5
sum	8.9	6.5	8.1	8.5	6.6	6.3

In summary, using a data sample of 4.479×10^8 $\psi(3686)$ events collected with the BESIII detector operating at the BEPCII collider, the decays $\psi(3686) \to e^+e^-\chi_{cJ}$ and $\chi_{cJ} \to e^+e^-J/\psi$ are observed for the first time, and the corresponding branching fractions are measured and the values are given in Table I. The ratios of branching fractions $\mathcal{B}(\psi(3686) \to e^+e^-\chi_{cJ})/\mathcal{B}(\psi(3686) \to \gamma\chi_{cJ})$ and $\mathcal{B}(\chi_{cJ} \to e^+e^-J/\psi)/\mathcal{B}(\chi_{cJ} \to \gamma J/\psi)$ are also obtained by incorporating the BESIII results of the product of branching fractions $\mathcal{B}(\psi(3686) \to \gamma\chi_{cJ})\mathcal{B}(\chi_{cJ} \to \gamma J/\psi)$ in Ref. [8], as listed in Table I. The common systematic uncertainties related to efficiency and branching fractions cancel in the calculation. The measured q^2 distributions are consistent with those of the signal MC simulation based on the assumption of a pointlike meson [20]. This first observation of the q^2-dependent charmonium EM Dalitz transitions can help understand the discrepancy between the experimental measurements [3] and the theoretical predictions [4–7] of the $\psi(3686) \to \gamma\chi_{cJ}$ branching fractions. The experimental methods applied here for the first study of charmonium Dalitz decays are likely to be of use for similar studies of the $X(3872)$. It is hoped that this experimental work will spur new theoretical development on the use of charmonium Dalitz decays to address questions such as the nature of exotic charmonium.

The BESIII Collaboration thanks the staff of BEPCII and the IHEP computing center for their strong support. This work is supported in part by National Key Basic Research Program of China under Contract No. 2015CB856700; National Natural Science Foundation of China (NSFC) under Contracts No. 11125525, No. 11235011, No. 11322544, No. 11335008, No. 11425524, No. 11521505, and No. 11575198; the Chinese Academy of Sciences (CAS) Large-Scale Scientific Facility Program; the CAS Center for Excellence in Particle Physics (CCEPP); the Collaborative Innovation Center for Particles and Interactions (CICPI); Joint Large-Scale Scientific Facility Funds of the NSFC and CAS under Contracts No. 11179007, No. U1232201, and No. U1332201; CAS under Contracts No. KJCX2-YW-N29 and No. KJCX2-YW-N45; 100 Talents Program of CAS; National 1000 Talents Program of China; INPAC and Shanghai Key Laboratory for Particle Physics and Cosmology; German Research Foundation DFG under Contracts No. Collaborative Research Center CRC-1044, No. FOR 2359; Istituto Nazionale di Fisica Nucleare, Italy; Koninklijke Nederlandse Akademie van Wetenschappen (KNAW) under Contract No. 530-4CDP03; Ministry of Development of Turkey under Contract No. DPT2006K-120470; Russian Foundation for Basic Research under Contract No. 14-07-91152; The Swedish Resarch Council; U.S. Department of Energy under Contracts No. DE-FG02-05ER41374, No. DE-SC-0010504, No. DE-SC0012069, and No. DESC0010118; U.S. National Science Foundation; University of Groningen (RuG) and the Helmholtzzentrum fuer Schwerionenforschung GmbH (GSI), Darmstadt; WCU Program of National Research Foundation of Korea under Contract No. R32-2008-000-10155-0.

[*]Corresponding author.
zhangjielei@ihep.ac.cn
[a]Also at State Key Laboratory of Particle Detection and Electronics, Beijing 100049, Hefei 230026, People's Republic of China.
[b]Also at Bogazici University, 34342 Istanbul, Turkey.
[c]Also at the Moscow Institute of Physics and Technology, Moscow 141700, Russia.
[d]Also at the Functional Electronics Laboratory, Tomsk State University, Tomsk, 634050, Russia.
[e]Also at the Novosibirsk State University, Novosibirsk, 630090, Russia.
[f]Also at the NRC "Kurchatov Institute", PNPI, 188300, Gatchina, Russia.
[g]Also at University of Texas at Dallas, Richardson, Texas 75083, USA.
[h]Also at Istanbul Arel University, 34295 Istanbul, Turkey.

[1] R. H. Dalitz, Proc. Phys. Soc. London Sect. A **64**, 667 (1951).
[2] L. G. Landsberg, Phys. Rep. **128**, 301 (1985).
[3] C. Patrignani *et al.* (Particle Data Group), Chin. Phys. C **40**, 100001 (2016).
[4] E. Eichten, K. Gottfried, T. Kinoshita, K. D. Lane, and T. M. Yan, Phys. Rev. D **21**, 203 (1980).
[5] N. Brambilla *et al.*, arXiv:hep-ph/0412158.
[6] T. Barnes, S. Godfrey, and E. S. Swanson, Phys. Rev. D **72**, 054026 (2005).
[7] Z. Cao, M. Cleven, Q. Wang, and Q. Zhao, Eur. Phys. J. C **76**, 601 (2016).
[8] M. Ablikim *et al.*, Phys. Rev. D **95**, 072004 (2017).
[9] R. T. Kleiv, T. G. Steele, A. Zhang, and I. Blokland, Phys. Rev. D **87**, 125018 (2013).
[10] Z. G. Wang and T. Huang, Phys. Rev. D **89**, 054019 (2014).
[11] L. Zhao, L. Ma, and S. L. Zhu, Phys. Rev. D **89**, 094026 (2014).
[12] O. Zhang, C. Meng, and H. Q. Zheng, AIP Conf. Proc. **1257**, 457 (2010).
[13] C. Meng, J. J. Sanz-Cillero, M. Shi, D. L. Yao, and H. Q. Zheng, Phys. Rev. D **92**, 034020 (2015).
[14] M. Ablikim *et al.* (BESIII Collaboration), Chin. Phys. C **37**, 063001 (2013).
[15] Using the same method as in Ref. [14], the total number of $\psi(3686)$ events taken at 2009 and 2012 is measured to be $(4.479 \pm 0.029) \times 10^8$ (to be published).
[16] M. Ablikim *et al.* (BESIII Collaboration), Nucl. Instrum. Methods Phys. Res., Sect. A **614**, 345 (2010).
[17] J. Z. Bai *et al.* (BESIII Collaboration), Nucl. Instrum. Methods Phys. Res., Sect. A **344**, 319 (1994); **458**, 627 (2001).
[18] M. Ablikim *et al.* (BESIII Collaboration), Chin. Phys. C **37**, 123001 (2013).
[19] D. J. Lange, Nucl. Instrum. Methods Phys. Res., Sect. A **462**, 152 (2001).
[20] A. Faessler, C. Fuchs, and M. I. Krivoruchenko, Phys. Rev. C **61**, 035206 (2000).

[21] S. Jadach, B. F. L. Ward, and Z. Was, Comput. Phys. Commun. **130**, 260 (2000); Phys. Rev. D **63**, 113009 (2001).
[22] J. C. Chen, G. S. Huang, X. R. Qi, D. H. Zhang, and Y. S. Zhu, Phys. Rev. D **62**, 034003 (2000).
[23] Z. R. Xu and K. L. He, Chin. Phys. C **36**, 742 (2012).
[24] M. Ablikim *et al.* (BESIII Collaboration), Phys. Rev. D **93**, 011102 (2016).
[25] M. Ablikim *et al.* (BESIII Collaboration), Phys. Rev. Lett. **116**, 251802 (2016).
[26] M. Ablikim *et al.* (BESIII Collaboration), Phys. Rev. D **87**, 012002 (2013).